DESIGN OF SINGLE PHASE GRID CONNECTED SOLAR PV INVERTER SYSTEM WITH ANFIS MPPT

Mohammad Ashar[1,2]*– Manjusha Palandurkar[1] – Pankaj Thote[2]

[1]Department of Electrical Engineering, Shri Ramdeobaba College of Engineering and Management, Nagpur, R.T.M.Nagpur University, Nagpur, Maharashtra, INDIA
[2]Department of Electrical Engineering, S.B. Jain Institute of Technology, Management & Research, Nagpur, R.T.M.Nagpur University, Nagpur Maharashtra, INDIA

ARTICLE INFO

***Article history*:**
Received: 14.12.2024.
Received in revised form: 22.01.2025.
Accepted: 12.03.2025.

Keywords:
Solar Energy
Photovoltaic
Maximum Power Point Tracking
Grid Synchronization
Single Phase
Grid inverter

DOI: https://doi.org/10.30765/er.2744

Abstract:

The application of single-phase grid-connected inverter systems is growing day by day, particularly in residential solar power generation. The systems are becoming popular as the rooftop solar PV solution of choice, due to the least infrastructure needs and lower installation expenses. Solar power generation is a variable process in terms of solar irradiation and ambient temperature. For maximum energy extraction from the PV modules, efficient Maximum Power Point Tracking (MPPT) techniques are vital. In this paper, the design, simulation, and performance analysis of a single-phase grid-connected solar photovoltaic (PV) inverter system using an Adaptive Network-Based Fuzzy Inference System (ANFIS) based MPPT technique is discussed. Conventional MPPT techniques, such as the Perturb and Observe (P&O) algorithm, are plagued with oscillations and sub-optimal tracking efficiency. As a counter measure, in this paper, an innovative 2.1 kW inverter system using ANFIS-based MPPT is developed to offer improved stability and efficiency in power extraction. The proposed system includes a solar PV array, a DC-DC boost converter designed with constant DC link voltage, and an H-bridge single-phase inverter synchronized with the grid through a Phase-Locked Loop (PLL) based control strategy. ANFIS controller is trained over vast datasets representing solar irradiance and temperature variations to develop an optimal reference voltage for the boost converter. MATLAB Simulink is utilized for simulation and comparison of the ANFIS-based MPPT performance with the conventional P&O technique. From the findings, it is clear that the ANFIS technique significantly reduces the oscillations in the PV panel voltage, current, and power, and hence saves energy losses and increases overall system efficiency. Under standard environmental condition and steady-state operation, the ANFIS-controlled system shows a stable PV panel voltage and an increase of 5.6% in grid-injected active power as compared with the P&O method. The system also shows improved performance with varying irradiance, affirming the adaptability of the ANFIS controller. The results indicate that use of ANFIS with grid-connected solar PV inverters can potentially improve performance significantly, opening the way for more efficient and reliable renewable energy integration into the contemporary power grid.

* Corresponding author
E-mail address:1069ashar@gmail.com

Nomenclature

ANFIS: Adaptive Network-Based Fuzzy Inference System
ANN: Artificial Neural Network
DC: Direct Current
INC: Incremental Conductance
LCL: Inductor-Capacitor-Inductor (filter)
MPPT: Maximum Power Point Tracking
P&O: Perturb and Observe
PI: Proportional-Integral (controller)
PLL: Phase-Locked Loop
PV: Photovoltaic
PWM: Pulse Width Modulation
SPWM: Sinusoidal Pulse Width Modulation
VSI: Voltage Source Inverter

1 Introduction

The world's shift to renewable energy systems has solidified the role of solar photovoltaic (PV) technology as an environmentally friendly solution to addressing increasing energy needs without contributing to more carbon emissions [1][2]. Grid-integrated PV systems, specifically, have been at the forefront of interest with scalability, decreased dependency on energy storage, and direct grid connection [3]. Efficiency and reliability of such systems, however, depend on two basic building blocks: (i) maximum power point tracking (MPPT) algorithms for maximum energy harvesting under time-varying environmental conditions, and (ii) power conversion and synchronization schemes to provide reliable grid integration under stringent power quality conditions [3][4]. Despite significant progress, achieving an optimal balance among tracking accuracy, dynamic performance, and overall system stability remains a challenge, particularly for single-phase grid-connected inverters in distributed systems. [5][6][7].

Conventional MPPT techniques, such as perturb-and-observe (P&O) and incremental conductance (INC), are still preferred because of ease of implementation and low computational effort [5][6][8]. Nonetheless, these methods continue to face fundamental challenges, including significant power drift in response to sudden variations in solar radiation, oscillations during steady-state operation, and inadequate performance under partial shading conditions. [5][8][9]. For instance, the conventional P&O technique suffers with drift errors during abrupt insolation increments [5][8]. Similarly, while INC offers greater precision in steady-state operation, the use of mathematical calculations increases the implementation complexity and hardware cost [9]. Modified step-size control and combined algorithms have been proposed in some studies in order to nullify these shortcomings, but oscillations and convergence remains the challenge[9] [10].

To address these challenges, intelligent MPPT techniques grounded in artificial intelligence (AI) have been introduced as robust alternatives. Adaptive Neuro-Fuzzy Inference Systems (ANFIS), with neural network learning capability and fuzzy logic interpretability, are promising for optimizing PV output under partial shading and varying weather conditions [11][12][13]. Unlike conventional techniques, ANFIS-based MPPT minimizes oscillations, enhances convergence, and dynamically adjusts to nonlinear PV behavior [11][12][14]. For example, [11] demonstrated ANFIS is the fastest algorithm, reduces power loss relative to P&O, while Worku and [12] validated its real-time effectiveness on dSPACE platforms. These findings demonstrate ANFIS as a potential solution towards energy extraction improvement in grid-connected systems [13][14].

Grid-connected inverter design is also a contributor to system performance, particularly for single-phase configurations in which synchronization, harmonic distortion, and voltage stability are issues of significant concern [1]][7] [15]. Conventional techniques of pulse-width modulation (PWM) and phase-locked loops (PLLs) are applied in voltage source inverters (VSIs), but transient stability and harmonic injection remain current concerns [7][15][16]. Advancements, such as sinusoidal pulse-width modulation (SPWM) with closed-loop voltage control, have led to greater harmonic suppression of single-phase inverters and improved efficiency [7]. Still, a combination of improvement of PLL design, e.g., incorporation of the rate-of-change-of-frequency (RoCoF) signals, enhances stability of the system [16]. Even so, convergence of such technology with AI-enpowered MPPT controllers is in its nascent stages, particularly in cost-limited small-scale applications[7] [15][17].

Although considerable progress has been achieved, existing solutions often treat MPPT and grid synchronization separately, exposing a clear gap that calls for a single, integrated framework merging both functionalities for more comprehensive analysis.This paper bridges this gap by offering a single-phase grid-connected solar PV inverter scheme with an ANFIS-based maximum power point tracking controller taking into account the individual strengths identified in the existing research literature.

The motivation behind this research arises from the need to integrate advanced MPPT methods with robust grid synchronization in single-phase solar PV systems, bridging the gap between maximizing power extraction and ensuring stable, high-quality power injection into the grid. Hence, the primary objective of this work is to develop and analyze a novel single-phase grid-connected solar PV inverter system equipped with an ANFIS-based MPPT controller, which is hypothesized to maximize energy extraction, reduce oscillations under varying irradiance conditions, and ensure stable grid integration compared to conventional methods. By combining robust power conversion capabilities with cutting-edge AI-driven MPPT, this work aims to boost both the efficiency and reliability of single-phase grid-connected PV systems, therefore contribute to the global move towards sustainable energy infrastructures.

The paper is organized as follows: Section-2 details the methodology behind the single-phase grid-connected solar PV inverter system incorporating both P&O and ANFIS-based MPPT techniques, while Section-3 explains the control strategies for MPPT and grid synchronization. Section 4 describes the MATLAB simulation model developed for this study, and Section 5 presents the simulation results. In Section 6, an in-depth analysis of the system's performance along-with practical considerations and limitations are discussed, and lastly, Section 7 concludes by summarizing the key findings and outlining future research directions.

2 Methodology

The block diagram of the work carried out is shown in Fig.1. It represents grid connected solar PV system which comprises of the solar PV modules rated for 2.1 kW, DC-DC boost converter for maintaining the DC link voltage at 400V, DC-AC Inverter for grid connection as well as to feed power in the grid. The synchronization circuit generates signals that control the gate drive circuit, thereby producing the SPWM output required to operate the single-phase H-bridge inverter. Phase Locked Loop (PLL) based technique was employed for single phase grid synchronization. For extracting maximum power from the solar PV modules, ANFIS and P&O MPPT algorithms were implemented to generate optimal duty ratio to control the conventional DC-DC boost converter. This DC-DC boost converter comprise of Inductor-Diode-MOSFET switch-Capacitor configuration working in continuous mode of operation as shown in Fig.7.

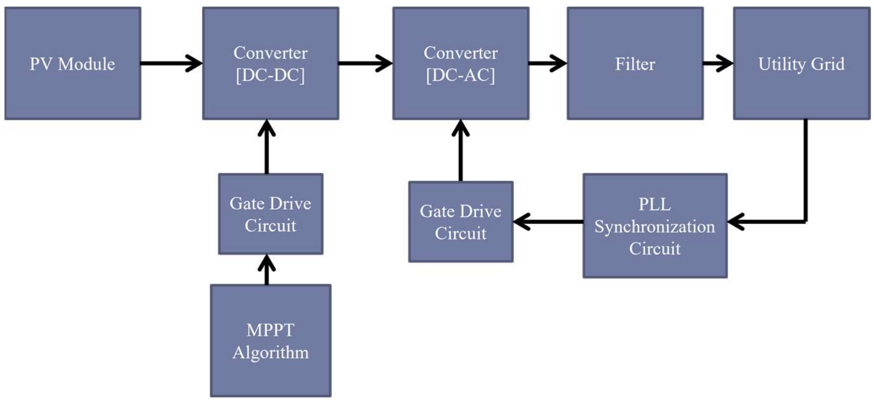

Fig. 1. Block diagram of grid connected solar PV System

The solar PV panel parameters and other components ratings are specified in the Appendix-I.

3 Control Strategy

3.1 MPPT Technique

3.1(a) Perturb and Observe method (P&O)

The maximum power point is reached by perturbing, observing and comparing the PV power. The current and voltage from PV panel (k^{th} instant) are sensed and hence, the PV power is obtained. Similarly, the power at different instances are calculated with the help of voltages and currents at those instances. The voltage and power at $(k+1)^{th}$ and kth instant is subtracted. On the right hand side of the curve of Fig. 2, power-voltage has a negative slope and on the left hand side it has a positive slope. The change in power with respect to change in voltage is calculated and the duty ratio is controlled so that the maximum power point is reached.

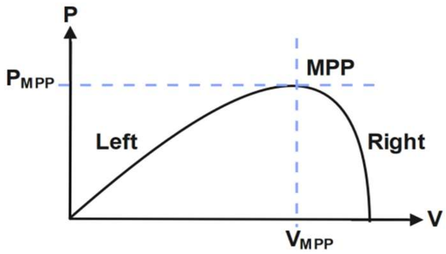

Fig. 2. PV characteristic curve of perturb and observe method

This method is based on the equation $\frac{dP}{dV}$ i.e. rate of change of power with respect to voltage

i. If $\frac{dP}{dV} > 0$, the duty cycle needs to be decreased in order to reach the maximum power point.
ii. If $\frac{dP}{dV} = 0$, then the PV voltage is said to be equal to the MPP voltage.
iii. If $\frac{dP}{dV} < 0$, then in order to achieve the Maximum Power Point, the duty cycle needs to be increased .[2]

When the maximum power point is reached, output power oscillates around the maximum power which leads to power loss. Due to this power loss it has low efficiency and tracking of maximum power point takes a long time.

3.1(b) ANFIS MPPT Control

For control of the MPPT employing ANFIS technique, the ANFIS model is trained with 1000 samples using two inputs i.e. Solar Irradiation and Ambient Temperature and the output is the reference voltage at the maximum power point. Using a PID controller, the actual PV voltage is compared against the ANFIS-generated reference MPP voltage to determine the duty cycle for the boost converter, thereby optimizing power output at the maximum power point.

In ANFIS method, it has the strengths of its two core methods i.e. Fuzzy Logic and Artificial Neural Networks (ANN). Fuzzy Logic translates qualitative human reasoning into precise, measurable analysis, while ANN excels in learning and adapting to changing conditions. By integrating ANN with Fuzzy Logic, ANFIS reduces error in defining rules, making the system more accurate. The ANFIS architecture is shown in Fig.3. [11]

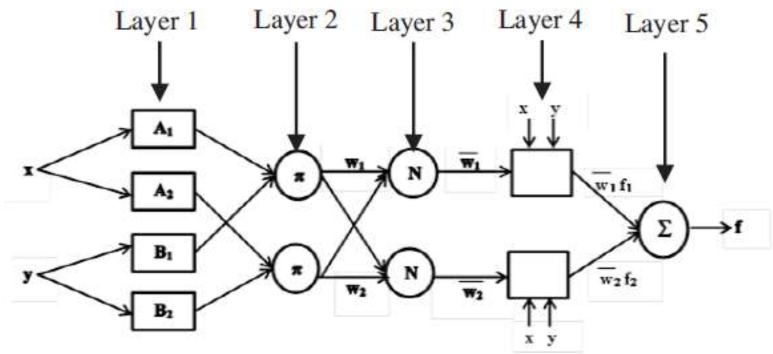

Fig. 3. ANFIS Architecture

ANFIS comprises of five layers-

Layer 1: Fuzzification Layer (Input Layer)
Each node in this layer represents a fuzzy membership function, which transforms each crisp input into a fuzzy value.
For each input **x** and membership function **A**, the output of each node in Layer 1 is given by: [11]

$$O_{1,i} = \mu_{A_i}(x) \tag{1}$$

$$O_{1,i} = \mu_{B_i}(y) \tag{2}$$

where:

- $\boldsymbol{\mu_{A_i}(x)}$ and $\boldsymbol{\mu_{B_i}(y)}$ are the membership functions of inputs **x** and **y** for fuzzy sets $\mathbf{A_i}$ and $\mathbf{B_i}$, respectively.
- The output $\boldsymbol{O_{1,i}}$ represents the degree of membership of the input to the fuzzy set.

Layer 2: Rule Layer (Product Layer)
Each node in this layer corresponds to a fuzzy rule and calculates the firing strength (weight) of each rule by multiplying the membership values from Layer 1.
For two inputs **x** and **y**, the firing strength $\mathbf{w_i}$ of rule **i** is: [11]

$$O_{2,i} = w_i = \mu_{A_i}(x) \cdot \mu_{B_i}(y) \tag{3}$$

This multiplication combines the memberships using the "AND" operation, commonly implemented as the product.

Layer 3: Normalization Layer
In this layer, the firing strengths from Layer 2 are normalized. Each node computes the ratio of a rule's firing strength to the total firing strengths, providing the normalized firing strength.
For each rule **i**, the normalized firing strength $\overline{w_i}$ is given by: [11]

$$O_{3,i} = \overline{w_i} = \frac{w_i}{\sum_j w_j} \tag{4}$$

where:

- $\boldsymbol{\sum_j \mathrm{v} w_j}$ is the sum of all firing strengths.
- This normalization ensures that the sum of all normalized firing strengths is 1.

Layer 4: Defuzzification Layer (Consequent Layer)
Each node in this layer computes the weighted output of each rule based on its normalized firing strength and a linear function.
The output of each node **i** in Layer 4 is: [11]

$$O_{4,i} = \overline{w_i} \cdot f_i \tag{5}$$

where $\mathbf{f_i}$ is a linear function: [11]

$$f_i = p_i x + q_i y + r_i \tag{6}$$

Here:

- p_i, q_i, and r_i are parameters that define the linear output function for each rule.
- These parameters are adjusted during the training process to minimize error.

Layer 5: Output Layer (Aggregation Layer)
This layer computes the overall output of the system by summing all the incoming signals from Layer 4.
The final output $\boldsymbol{O_5}$ of the ANFIS model is: [11]

$$O_5 = \sum_i \overline{w}_i \cdot f_i \tag{7}$$

This final output represents the overall prediction or decision of the ANFIS system, calculated as the weighted sum of each rule's output.

In the designed ANFIS controller, the Input1 is the irradiance in W/m^2, Input2 is the Temperature in ºC and output is the voltage at maximum power point in volts. The rule and surface view of the ANFIS controller is shown in Fig. 4 and Fig.5 respectively.

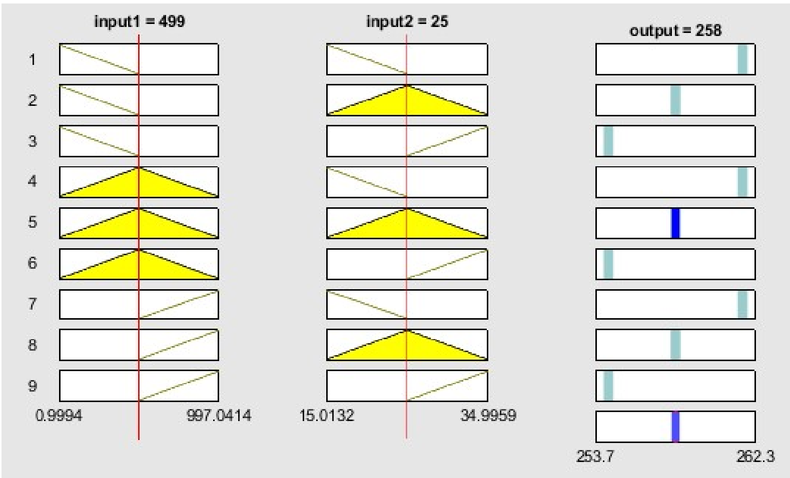

Fig. 4. Rule view of ANFIS controller

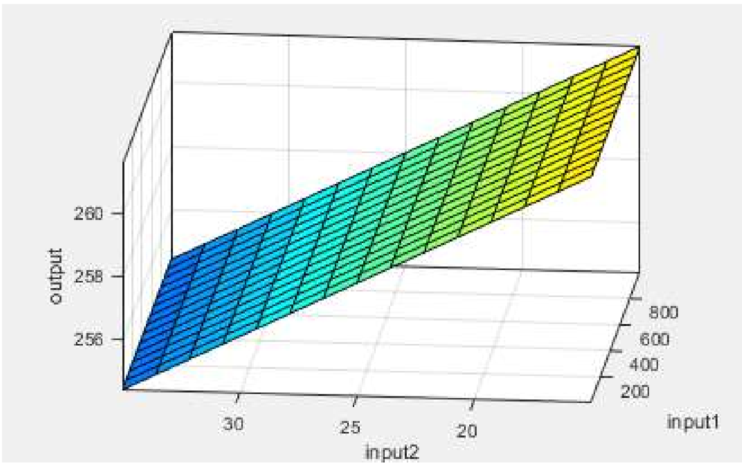

Fig. 5. Surface view of ANFIS controller

3.2 PLL based Grid Synchronization

The Grid connected Inverters mostly rely on phase locked loop (PLL) for synchronization with the grid[16]. In this work, a synchronous reference frame Phase-Locked Loop(SRF-PLL) synchronization is employed for the single phase grid connected model for synchronization with grid voltage, the details are as provided below-

The input to the PLL is the grid voltage v_g, represented as:

$$v_g = V_m \sin(\omega t + \phi) \tag{8}$$

Where-
$\boldsymbol{V_m}$: The peak voltage of the grid.
ω: The angular frequency of the grid (rad/s).
ϕ: The phase of the grid voltage.

Generation of a Quadrature Signal:

A quadrature signal with 90-degree phase-shift of the input signal, denoted as $v_{g,q}$ is generated by passing the input signal through two low pass filters and gain adjusted for maintaining the same amplitute.

$$v_{g,q} = V_m \cos(\omega t + \phi) \tag{9}$$

Park Transformation:

The two signals, v_g and $v_{g,q}$, are transformed into the **dq rotating reference frame** using the following equations:

$$v_d = v_g \cos(\theta) + v_{g,q} \sin(\theta) \tag{10}$$

$$v_q = -v_g \sin(\theta) + v_{g,q} \cos(\theta) \tag{11}$$

v_d: Represents the voltage component aligned with the reference angle θ.
v_q: Represents the quadrature voltage (orthogonal to θ).

Here, $\theta=\int\omega_{pll}\, dt$ is the estimated phase from the PLL which the PLL continuously adjusts to match the grid phase ϕ.

Error Detection:

The v_q signal indicates how far the PLL's phase (θ) is from the grid phase (ϕ). Initially:

$$v_q = -V_m \sin(\phi - \theta) \tag{12}$$

When ϕ=θ (perfect synchronization), $v_q = 0$
If ϕ≠ θ, v_q is nonzero, and its sign indicates whether θ is leading or lagging.

The PLL operates by driving v_q to zero, ensuring synchronization.

Proportional-Integral (PI) Controller:

The error signal v_q is passed through a Proportional-Integral (PI) controller to adjust the estimated angular frequency ω_{pll}:

$$\omega_{pll} = K_p v_q + K_i \int v_q \, dt \tag{13}$$

where Kp and Ki are the proportional and integral gains of the PI controller.

Phase Estimation:

The phase θ(calculated by integrating ω_{pll}) is the PLL's best estimate of the grid phase ϕ. Once v_q is zero, the PLL is synchronized, and θ matches ϕ.
The estimated phase θ is obtained by integrating ω_{pll}:

$$\theta = \int \omega_{pll} \, dt \tag{14}$$

3.3 Maintaining DC Bus Voltage (Vdc)constant :

The DC bus voltage (vdc) is regulated to the desired value i.e. 400V using a PI controller.

$$e(t) = V_{dc\_ref} - V_{dc} \tag{15}$$

Where:

- $V_{dc\_ref} = 400$ V
- $V_{dc}$is the actual measured DC voltage.

The PI controller generates a control signal $iref(t)$, which represents the required sinusoidal current that the inverter must inject into the grid:

$$iref(t) = Kp * e(t) + Ki \int e(t) \, dt \tag{16}$$

Where:

- Kp and Ki are proportional and integral gains, respectively.

This ensures the DC bus voltage remains close to the desired value.

This $i_{ref}(t)$ is multiplied with Grid Voltage Reference (cosωt) to ensure that the current injected into the grid is synchronized in phase with the grid voltage.

3.4 PR Controller for Current Regulation :

The Proportional-Resonant (PR) controller ensures that the current injected into the grid by the inverter matches the sinusoidal reference signal $i_{ref}(t)$.
The PR controller equation is given by:

$$GPR(s) = K_p + \frac{K_r s}{s^2 + \omega^2} \tag{17}$$

Where:
Kp is the proportional gain.
Kr is the resonant gain.
ω=2πf is the angular frequency.
This controller provides high gain at the fundamental grid frequency (50 Hz) to track sinusoidal references with minimal error.

The output of the PR controller is used to calculate the reference voltage V_{ref} for the SPWM.

3.5 SPWM for H-Bridge Inverter

The generated V_{ref} is used in the SPWM (Sinusoidal Pulse Width Modulation) technique to control the switching of the H-bridge inverter. The H-bridge generates a high-frequency PWM signal as shown in Fig. 6 that matches the amplitude, phase, and frequency of V_{ref} .

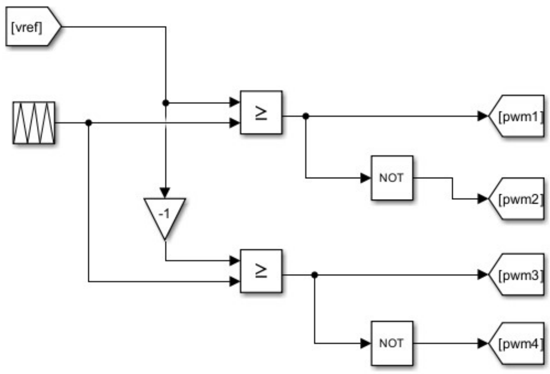

Fig. 6. Surface view of ANFIS controller

These PWM signals regulate the IGBT switches in the inverter, allowing it to produce a sinusoidal output that is synchronized with the grid. The SPWM technique ensures that the inverter delivers power to the grid smoothly and efficiently, with minimal harmonic distortion [7]. By adjusting the pulse width in response to the reference signal, the inverter can match the grid's voltage and phase, ensuring proper synchronization and maximizing power transfer.

4 MATLAB Simulink Model

The generalized simulation model of the work carried out is shown in Fig. 7.

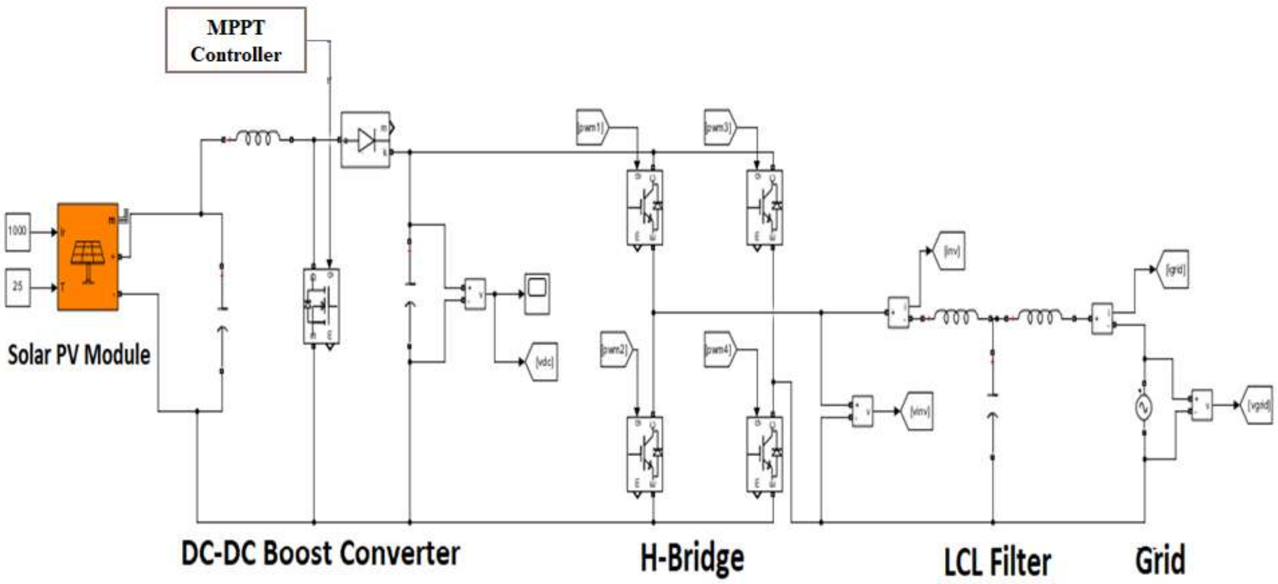

Fig. 7. Generalized simulation model of grid connected single phase Inverter system

The model consists of a solar PV array, a DC-DC boost converter, a single-phase H-bridge inverter connected to the grid via LCL. The boost converter tracks the maximum power point (MPPT) and steps up the solar PV voltage to maintain the DC link voltage at an appropriate level. The LCL filter removes harmonics, while the inverter is synchronized with the grid using a phase-locked loop (PLL), feeds active power to the grid.

The solar PV array includes six panels connected in series to achieve the voltage and power ratings as specified in Annexure-I. This configuration ensures compatibility with the system's design parameters.

The DC-DC boost converter comprises a boosting inductor, a forward diode that prevents reverse current flow, and an IGBT switch controlled by PWM pulses from the MPPT controller. This setup optimizes power extraction from the solar PV array while stepping up the voltage as required.

The single-phase H-bridge inverter consists of four IGBT switches connected to the 230V, 50 Hz grid through the LCL filter. The inverter output is synchronized with the grid using the PLL technique and Sine PWM for generation of output voltage. Maximum power point tracking is implemented using the P&O and ANFIS algorithms as shown in Fig. 8 and Fig. 9 respectively to ensure efficient energy transfer.

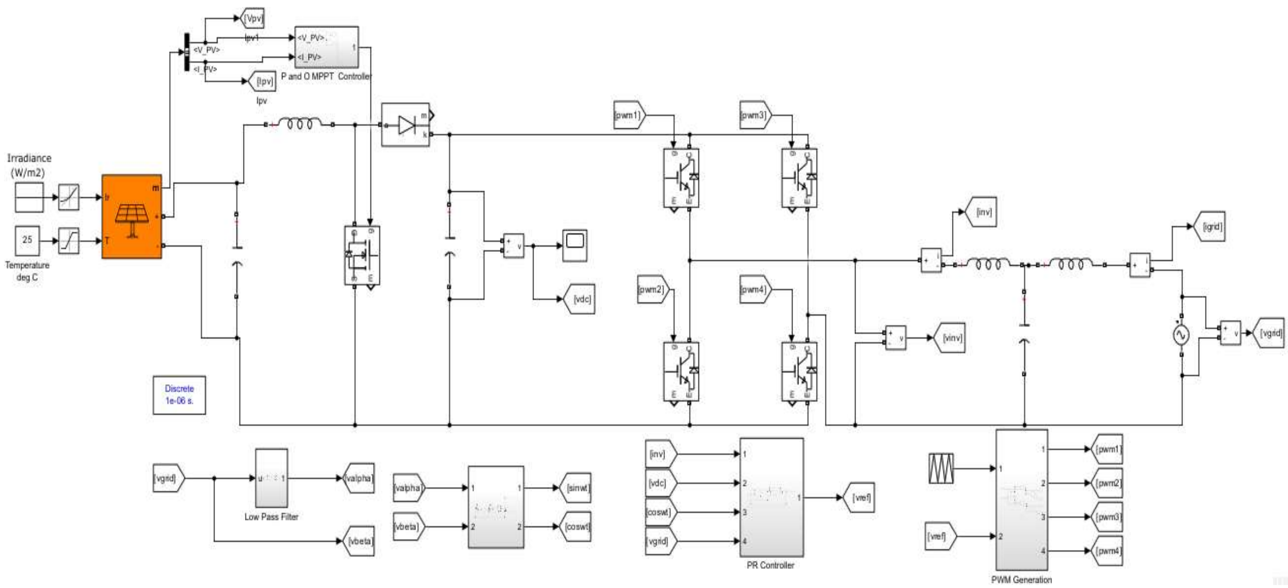

Fig. 8. MATLAB simulation model of grid connected single phase Inverter system with P&O MPPT

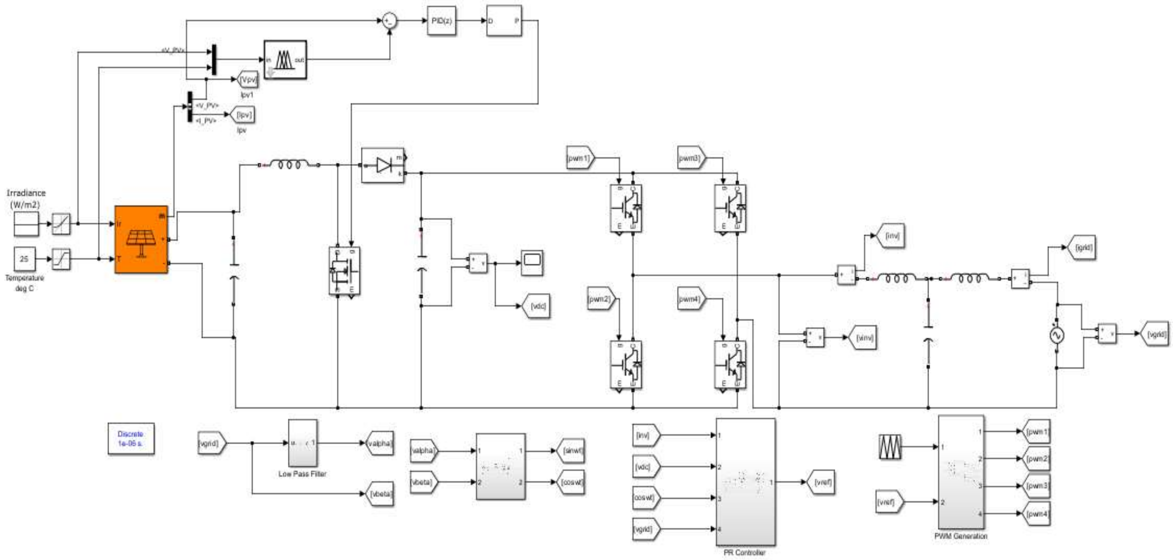

Fig. 9. MATLAB simulation model of grid connected single phase Inverter system with ANFIS MPPT

5 Results

5.1 Performance of Inverter under steady state condition.

The simulation was carried with standard solar irradiance of 1000 W/m2, temperature 25 deg. C and the nature of PV Panel Voltage, PV Output Current, Solar PV Power, Grid and Inverter Voltages and Currents and Grid Injected Power for both P&O and ANFIS techniques are recorded and presented.

MPPT- P&O	**MPPT- ANFIS**
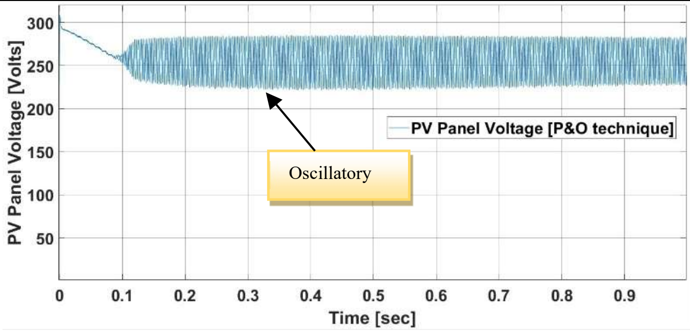	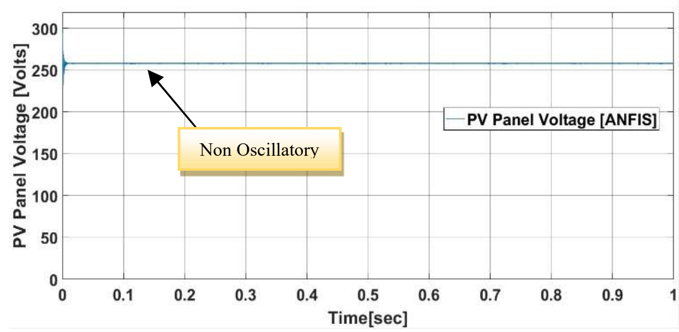
Fig. 10 (a) Solar PV Panel Voltage with P&O MPPT	*Fig. 10 (b) Solar PV Panel Voltage with ANFIS MPPT*
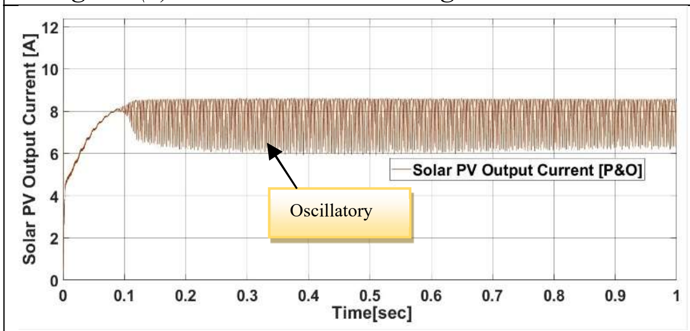	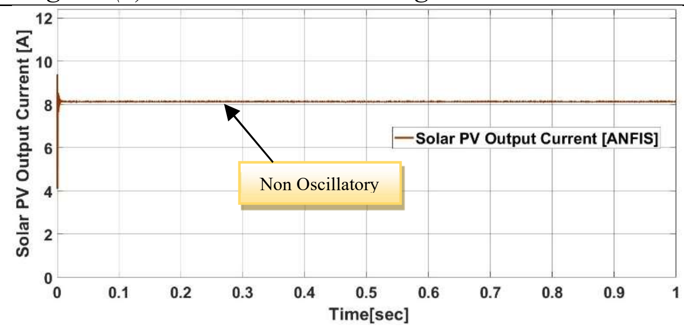
Fig. 11 (a) Solar PV Panel Current with P&O MPPT	*Fig. 11 (b) Solar PV Panel Current with ANFIS MPPT*
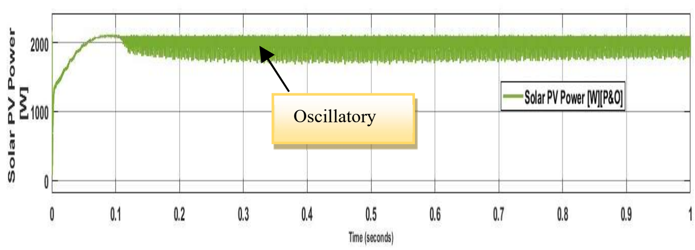	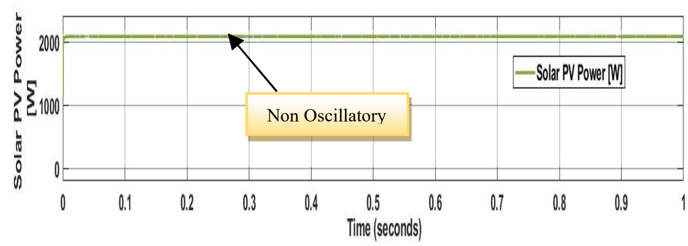
Fig. 12 (a) Solar PV Power with P&O MPPT	*Fig. 12 (b) Solar PV Power with ANFIS MPPT*

Table 1 Comparison of Solar PV Panel Voltage, Current and Power between P&O and ANFIS MPPT

Parameter	**P&O MPPT**	**ANFIS MPPT**
Solar PV Panel Voltage	225V - 283V [Oscillatory]	258V [Steady]
Solar PV Panel Current	6.1A- 8.6A [Oscillatory]	8.13A [Steady]
Solar PV Power	1740W – 2100W [Oscillatory]	2097W [Steady]

With P&O technique, solar PV Panel Voltage oscillates between 225V and 283V as shown in Fig. 10(a), solar PV Output Current oscillates between 6.1A and 8.6A as shown in Fig. 11(a) and the solar PV Output Power oscillates between 1740W and 2100W as shown in Fig. 12(a). Whereas, with ANFIS MPPT, solar PV

Panel Voltage is settled at 258V as shown in Fig. 10(b), solar PV Output Current settled at 8.13A as shown in Fig. 11(b) and the solar PV Output Power is settled at 2097W as shown in Fig. 12(b).

MPPT- P&O

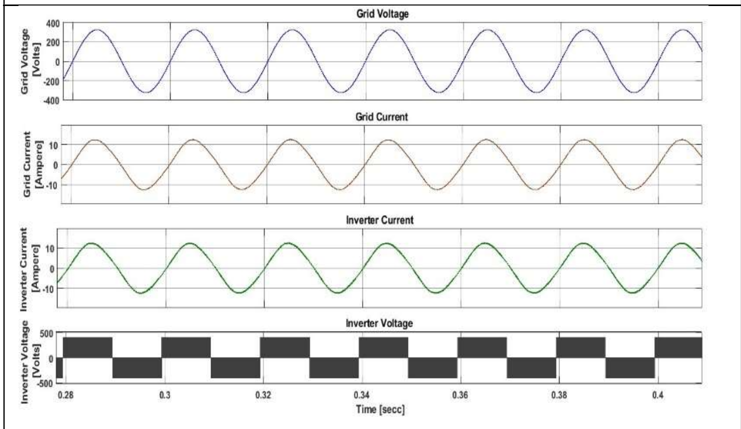

Fig. 13 (a) Grid and Inverter Voltage and Current with P&O MPPT

MPPT- ANFIS

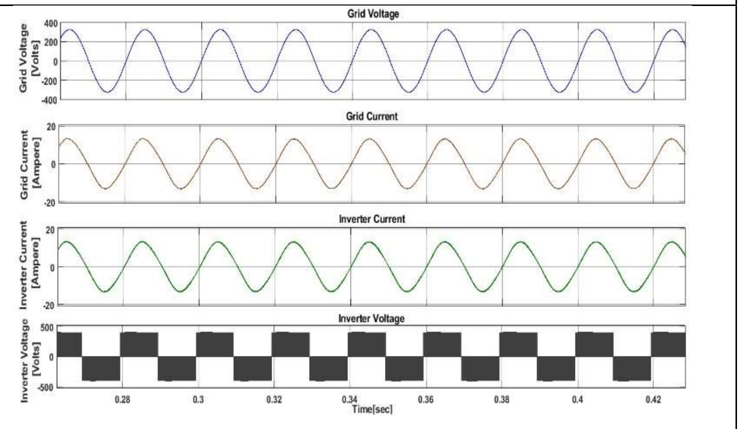

Fig. 13 (b) Grid and Inverter Voltage and Current with ANFIS MPPT

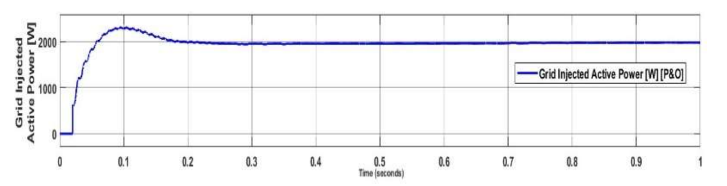

Fig. 14 (a) Grid Injected Active Power with P&O MPPT

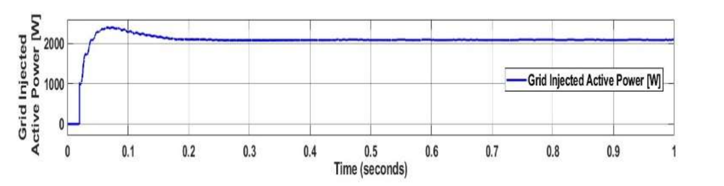

Fig. 14 (b) Grid Injected Active Power with ANFIS MPPT

Table 2 Comparison of Grid Injected Active Power between P&O and ANFIS MPPT

Parameter	P&O MPPT	ANFIS MPPT
Grid Injected Active Power	1980W	2090W

Grid and Inverter Voltage & Current waveform under steady state condition with P&O and ANFIS MPPT is shown in Fig. 13(a) and 13(b) respectively. With P&O MPPT, Grid Injected Active Power is 1980W as shown in Fig. 14(a) and with ANFIS MPPT, Grid Injected Active Power is 2090W as shown in Fig. 14(b). The experimental results demonstrate that the ANFIS-based MPPT method enhances grid-injected active power by **5.6%** compared to the conventional P&O technique under identical operating conditions.

The results highlight that the ANFIS MPPT method delivers a more stable and efficient performance compared to the P&O MPPT approach. With ANFIS, the solar PV panel voltage and current remains steady, resulting in a consistent power output. In contrast, the P&O method shows oscillations in both voltage and current, leading to an oscillatory power output. These fluctuations in the P&O approach can cause inefficiencies, as the system frequently deviates from the maximum power point.

5.2 Performance of Inverter under dynamic condition.

To assess the inverter's performance under dynamic conditions, the irradiance was varied to simulate both increasing and decreasing scenarios. The simulation began with an irradiance of 500 W/m², which was then raised to 1000 W/m² at 1 second and reduced to 800 W/m² at 2 seconds. The circuit was simulated over a total duration of 3 seconds. Figures 15(a) and 15(b) illustrate the inverter and grid voltages & currents for P&O and ANFIS techniques respectively and Figure 16 compares the grid-injected power of P&O and ANFIS technique.

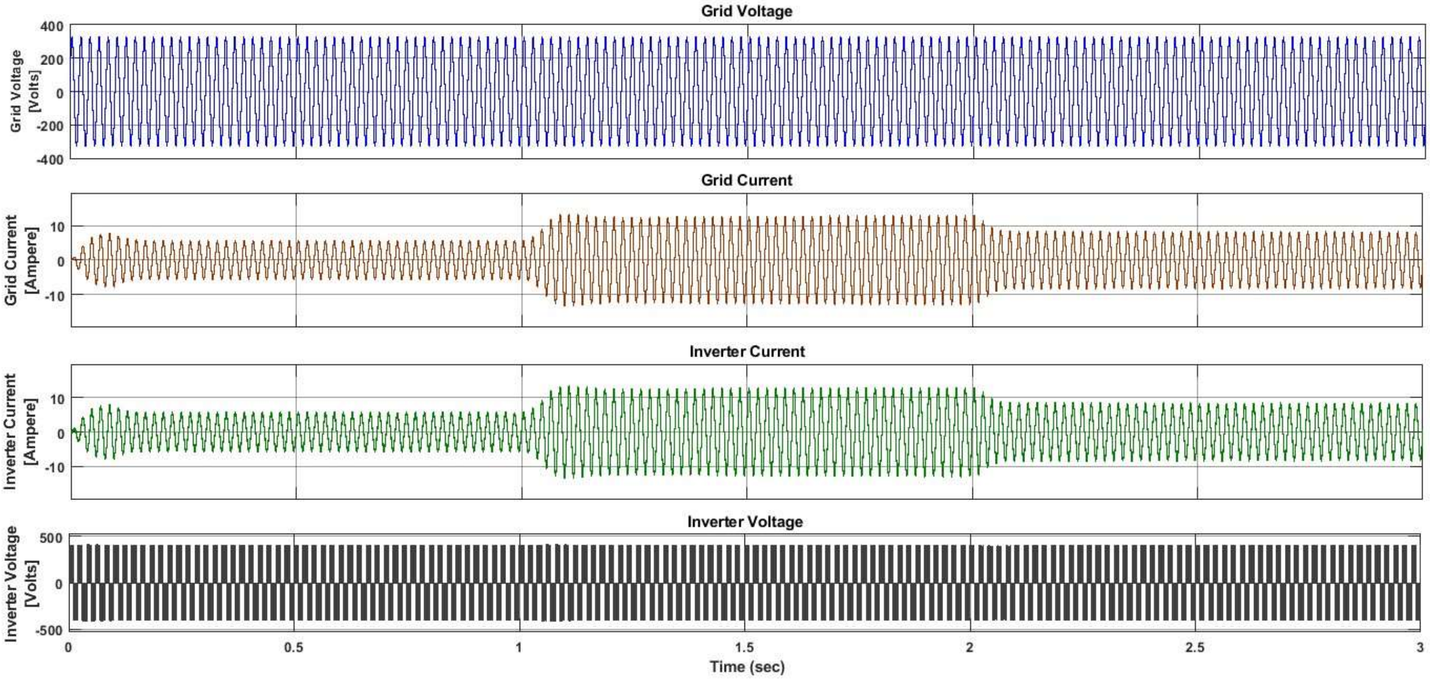

Fig. 15(a) Grid and Inverter Voltage & Current with P&O MPPT under dynamic condition

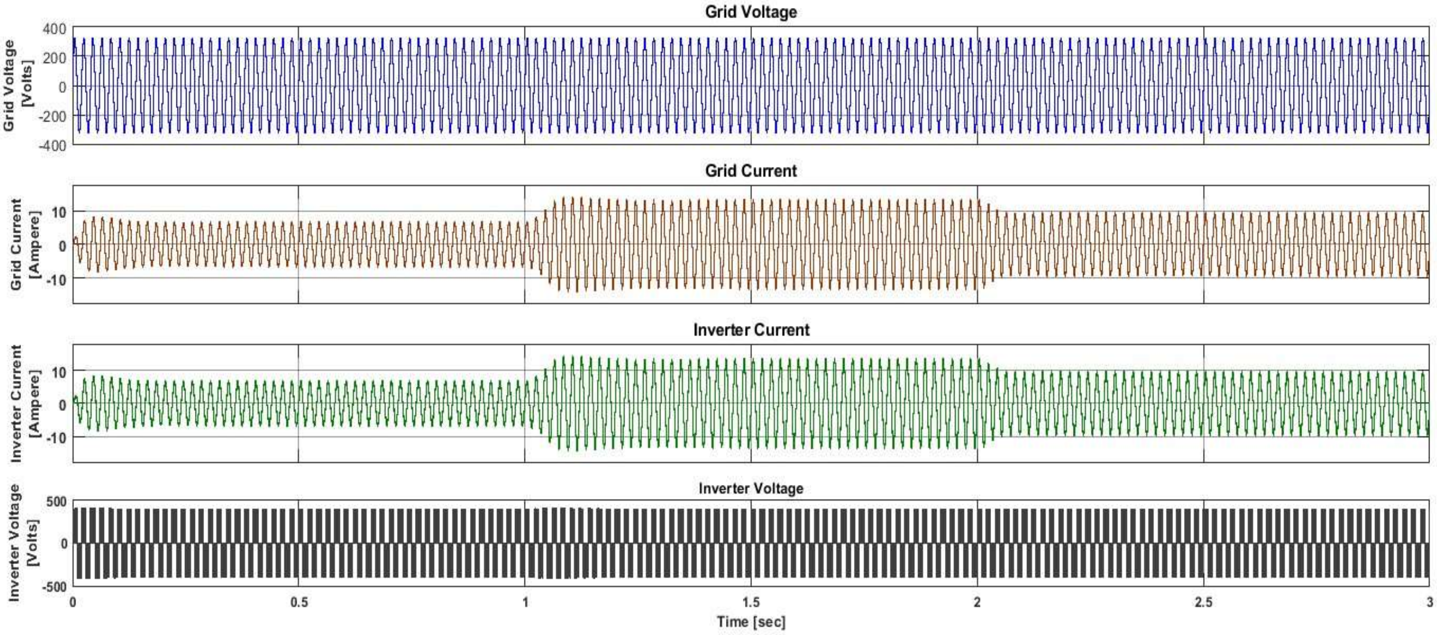

Fig. 15(b) Grid and Inverter Voltage & Current with ANFIS MPPT under dynamic condition

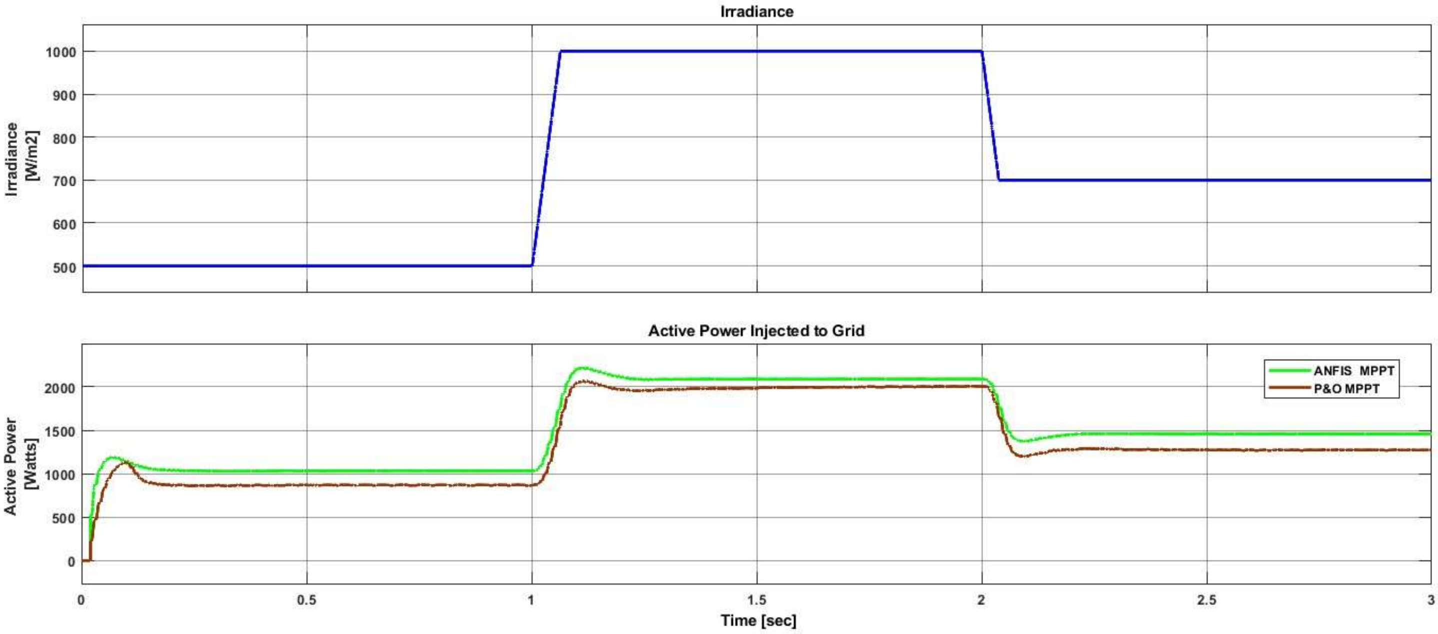

Fig. 16 Grid injected power with P&O and ANFIS MPPT under Dynamic Condition

The result confirms that both P&O and ANFIS techniques effectively regulate inverter performance under dynamic irradiance variations, maintaining stable inverter and grid voltage-current profiles. Notably, the power injected by ANFIS was significantly higher compared to P&O.

6 In-Depth Analysis and Discussion

The experimental results of Section 5 confirm the improved performance of the ANFIS-based MPPT controller over the conventional P&O algorithm. This section presents the technical and practical implications of these finding as well as discusses limitations and prospects for future directions.

6.1 ANFIS-Based Stability and Efficiency Improvement

The steady-state responses (Table 1) demonstrate that the ANFIS controller eliminates voltage and current oscillations observed in the P&O method. This stability arises because ANFIS can dynamically adapt to environmental variations through its hybrid neural-fuzzy architecture, which combines the learning capability of artificial neural networks (ANN) with the interpretability of fuzzy logic rules. Compared to P&O that relies on iterative perturbations to track the MPP, ANFIS generates an ideal reference voltage from irradiance and temperature readings which minimizes transient errors.

The ANFIS method results in a higher and more stable grid-injected active power, compared to the P&O method.The 5.6% power injection increase into the grid (Table 2) points towards the practical use of ANFIS in increasing the energy production. This makes ANFIS a better and effective solution for rooftop solar PV systems from the point of view of stability and efficient power injection into the grid.

The simulation results are encouraging but in practice, the ANFIS model would need to be optimized to strike a balance between accuracy and computational expense.

6.2 Dynamic Performance and Adaptability

At varying irradiance levels (Figs. 15–16), the ANFIS controller exhibited robust synchronization with the grid with greater power output than P&O. Such adaptability is necessary for rooftop PV systems, where transient cloud cover and partial shading are the occurances. ANFIS pre-trained inference function allows for quicker convergence to the MPP since it is able to forecast best operating points using patterns in past data.

6.3 Limitations and Practical Considerations

While the suggested system is promising, there are some limitations that need to be worked on. First, the training of the ANFIS model was based on a sample size of 1,000 under perfect test conditions. Real-world implementations with uncertain weather or non-uniform shading may demand larger and more diverse training data sets to provide robustness. Second, the simulation is under perfect grid conditions, ignoring harmonics or voltage unbalance that in real grids would impact synchronization. The system may be tested in future studies under non-ideal grid conditions, i.e., frequency-varying weak grids, to establish the robustness of the PLL.

7 Conclusion

The work demonstrates that the single-phase grid-connected solar PV inverter system integrated with an ANFIS-based MPPT technique exhibits superior performance over the conventional P&O method under both steady-state and dynamic conditions. Under steady-state conditions, while the P&O method resulted in oscillatory PV panel voltage, current and power, the ANFIS technique maintained steady values of these parameters. This stability not only reduces energy losses but also results in more efficient power delivery, as evidenced by the 5.6% higher grid-injected active power with ANFIS MPPT as compared with P&O technique under identical conditions.

Furthermore, under dynamic operations—where irradiance varied in ramp-up and ramp-down situations, the inverter system continued to exhibit strong performance. Both MPPT strategies effectively regulated the inverter and grid voltages and currents; however, ANFIS consistently injected significantly higher power into the grid, reflecting its superior control capability. The novelty of this work lies in its integration of an ANFIS-based MPPT controller with a single-phase grid-connected inverter, yielding improved energy extraction, reduced oscillations, and enhanced reliability compared to conventional methods. The findings in the work strongly support the hypothesis that ANFIS-based MPPT not only addresses the inherent variability of solar power generation more effectively but also paves the way for enhanced grid integration and microgrid stability. The limitations include the implementation in real world environment and future work should focus on experimental validation of the proposed model under real-world operating conditions to confirm its performance and reliability.

References

[1] Manjusha Palandurkar and Mohan M Renge, "Development of Grid Tied Inverter for Indian Grid and Operating Environmental Condition" The Electrochemical Society, ECS Transactions, Volume 107, Number 1, 2022.

[2] M. H. Mohamed Hariri, M. K. Mat Desa, S. Masri, and M. A. A. Mohd Zainuri, "Grid-Connected PV Generation System—Components and Challenges: A Review," Energies, vol. 13, no. 17, p. 4279, Aug. 2020.

[3] Ali Q. Al-Shetwi, M A Hannan, Ker Pin Jern, Ammar A. Alkahtani and A. E. PG Abas, "Power Quality Assessment of Grid-Connected PV System in Compliance with the Recent Integration Requirements", MDPI Electronics 2020, 9, 366.

[4] Fatima Zohra Kebbab, Louarem Sabah, Hamou Nouri, "A Comparative Analysis of MPPT Techniques for Grid Connected PVs", Engineering, Technology & Applied Research, Vol. 12, No. 2, pp. 8228–8235, 2022.

[5] M. Killi and S. Samanta, "Modified Perturb and Observe MPPT Algorithm for Drift Avoidance in Photovoltaic Systems," IEEE Trans. Ind. Electron., vol. 62, no. 9, pp. 5549–5559, Sept. 2015.

[6] D. Sera, L. Mathe, T. Kerekes, S. V. Spataru and R. Teodorescu, "On the Perturb-and-Observe and Incremental Conductance MPPT Methods for PV Systems," IEEE J. Photovoltaics, vol. 3, no. 3, pp. 1070–1078, July 2013.

[7] Xianglu Guo, Juanjuan Li, and Lexiao Peng, "Design of SPWM-based Single-phase Voltage Stabilized Inverter," 7th International Conference on Electronics, Communications, and Control Engineering (ICECC), IEEE, 2024, DOI: 10.1109/ICECC63398.2024.00017.

[8] Elbaset, H. Ali, M. Abd-El Sattar and M. Khaled, "Implementation of a Modified Perturb and Observe Maximum Power Point Tracking Algorithm for Photovoltaic System Using an Embedded Microcontroller," IET Renewable Power Gener., vol. 10, no. 4, pp. 551–560, April 2016.

[9] N. E. Zakzouk, M. A. Elsaharty, A. K. Abdelsalam, A. A. Helal and B. W. Williams, "Improved Performance Low-Cost Incremental Conductance PV MPPT Technique," IET Renewable Power Gener., vol. 10, no. 4, pp. 561–574, April 2016.

[10] J. Liu, J. Li, J. Wu and W. Zhou, "Global MPPT Algorithm with Coordinated Control of PSO and INC for Rooftop PV Array," J. Engineering, vol. 2017, no. 13, pp. 778–782, 2017.

[11] K. Amara, A. Fekik, D. Hocine, M. L. Hamida, E.-B. Bourennane, T. Bakir, and A. Malek, "Improved Performance of a PV Solar Panel with Adaptive Neuro Fuzzy Inference System (ANFIS) Based MPPT," 7th International Conference on Renewable Energy Research and Applications, Oct. 2018.

[12] Muhammed Y. Worku and M.A. Abido, "Grid Connected PV System Using ANFIS Based MPPT Controller in Real Time," Renewable Energy and Power Quality Journal.

[13] Arafat Ibne Ikram et al., "A Grid-Connected ANFIS-MPPT Based Solar PV System and Hybrid Energy Storage," in Proceedings of the 2023 IEEE 9th International Women in Engineering (WIE) Conference on Electrical and Computer Engineering (WIECON-ECE), Nov. 2023.

[14] Siddaraj SIddaraj, Udaykumar R. Yaragatti, and Nagendrappa Harischandrappa, "Coordinated PSO-ANFIS-Based 2 MPPT Control of Microgrid with Solar Photovoltaic and Battery Energy Storage System," Journal of Sensor and Actuator Networks, vol. 12, no. 3, Article 45, 2023.

[15] Pemendra Kumar Pardhi, Student Member, IEEE, Shailendra Kumar Sharma, Senior Member IEEE, and Ambrish Chandra, Fellow, IEEE, "Control of Single Phase Solar Photovoltaic Supply System", IEEE Transactions on Industry Applications, 2020.

[16] Abdullah M. Abusorrah and Hamed Sepahvand, "Enhancing Stability in Single-Phase PLLs: Incorporation of RoCoF Signal in Virtual Orthogonal Signal Construction," IEEE Transactions on Industrial Electronics, Vol. 71, Issue: 8, Aug. 2024.

[17] M. Fannakh, M. L. Elhafyani and S. Zouggar, "Hardware Implementation of the Fuzzy Logic MPPT in an Arduino Card Using a Simulink Support Package for PV Application," IET Renewable Power Gener., vol. 13, no. 3, pp. 510–518, Feb. 2019

.

Appendix-I

Ratings of 1Φ Grid Tied Solar PV System

S.No.	Particular	Details
1	Total KW rating	2.1 KW
2	No. of Parallel strings	1
3	Series-connected modules per string	6
4	Maximum Power (W) per module	349.59W
5	Open circuit voltage Voc (V) per module	51.5V
6	Short-circuit current Isc (A) per module	9.4A
7	Voltage at maximum power point Vmp (V) per module	43V
8	Current at maximum power point Imp (A) per module	8.13A
9	Standard Radiation	1000W/m2
10	Standard Temperature	25 degree
11	DC-DC Boost Converter Inductor	20 mH
12	DC Bus Capacitor	3000 μF
13	LCL Filter Inductor	10 mH each
14	LCL Filter Capacitor	0.5 μF
15	DC Bus Voltage	400V
16	Grid	1 Phase, 230V, 50Hz